**Title:** Targeted integration of extrachromosomal arrays in *C. elegans* using PhiC31 integrase

**Authors:** Matthew S. Rich[1], Ryan Pellow[1], Adam Hefel[1], Ofer Rog[1], Erik M. Jorgensen[1,2]
**Affiliations:** 1 – Department of Biology, University of Utah; 2 – HHMI
Corresponding author: EMJ jorgensen@biology.utah.edu

**Abstract**

Extrachromosomal arrays are unique chromosome-like structures created from DNA injected into the *C. elegans* germline. Arrays are easy to create and allow for high expression of multiple transgenes. They are, however, unstable unless integrated into a chromosome. Current methods for integration, such as X-rays and CRISPR, damage DNA and are low-efficiency. Here, we demonstrate that the viral integrase PhiC31, which mediates a non-mutagenic recombination between short *attB* and *attP* sequences, can be used for extremely efficient and targeted integration of arrays.

In this method, a transgene, a selectable marker, and *attP* sites are injected into the gonad of a strain that (1) has an *attB* site in its genome, and (2) expresses PhiC31 in its germline. F1 extrachromosomal arrays are cloned, grown for multiple generations with selection, and then screened for homozygous array integrations. The procedure is simple, requires less time than screening for extrachromosomal arrays, and arrays can be screened for transgene function after stable integration. Arrays that transmit are integrated by PhiC31 with 50-95% efficiency, allowing for the isolation of many unique integrants from a single injection. Arrays can also be integrated at fluorescent landing pads and arbitrary sites in the genome. Using nanopore sequencing, we show that three new integrated arrays are between 1.6 and 18 megabases in length, assemble with large repeats, and can contain hundreds of copies of injected transgenes. We have built a collection of strains and plasmids to enable array integration at multiple sites in the genome using various selections. PhiC1-mediated Integration of Arrays of Transgenes (PhiAT) will allow *C. elegans* researchers to shift from using unstable extrachromosomal arrays to directly integrating arrays.

## Introduction

Extrachromosomal arrays are the workhorse of *C. elegans* transgenesis. These miniature chromosomes provide a simple, rapid and efficient way to overexpress transgenes; injecting a worm gonad with a DNA mix can yield dozens of unique mini chromosomes that segregate across cell divisions and generations (*1*). Injected DNA concatenates via homologous recombination and non-homologous end-joining (*2*, *3*) into a megabase-scale circular mini-chromosome (*4*). Arrays form after fertilization, mature over the course of the first few cell divisions and are actively, but not perfectly, segregated by kinetochore proteins (*5*).

Because extrachromosomal arrays can be somatically lost and don't follow Mendelian segregation, *C. elegans* geneticists have developed methods to integrate these giant molecules into the genome where they will be faithfully segregated. All current methods for integrating extrachromosomal arrays require DNA damage: double-stranded DNA breaks in both the genome and the array can be repaired by inserting the array into the genome. The most commonly used method to induce breaks is through irradiation (*6*, *7*). In this method, extrachromosomal arrays are selected which have a transmission rate much less that 75%, then irradiated. Since integration is only ~1-5% efficient, hundreds of F1 progeny are cloned and screened for 75% array transmission, indicating a heterozygous array in the genome. Those strains are then homozygosed to create a single integrated line. Irradiation breaks the genome very effectively, but randomly; arrays are integrated at random positions in the genome and must be mapped genetically. In addition, it is common for strains with arrays integrated by irradiation to have background mutations, ranging in size and severity from point mutations to chromosomal translocations. While many of these can be crossed out of the strain, because the endpoints of the integration site are often scrambled, it may be impossible to remove all background mutations.

The advent of CRISPR technologies enabled targeted integration that is less mutagenic than irradiation. Most methods create a double-stranded break in the genome (now at a single site of your choosing) and in the array (at potentially many targets encoded in the DNA that was injected) (*8*, *9*). After introducing DNA breaks by CRISPR, various screening and selection strategies have been employed to isolate integrants. Targeting an endogenous gene provides a phenotypic selection; screening, for instance, for array(+) Dpys for arrays integrated at *dpy-3* or for array(+) benomyl-resistance for arrays integrated at *ben-1* (8). Fluorescent transgenes can be used as landing pads; integration knocks out the fluorescent protein, so integrants are isolated as array(+) and otherwise non-fluorescent (*10*). Alternatively, landing pads can be engineered with a split selectable marker for positive selection; for instance, unc-119(+) rescue occurs only when an array is integrated at the landing pad (*9*). Across the board, whether using X-rays or CRISPR, the efficiency of integration is low: generally between ~1-10% of animals after the integration process contain an integrated array in their

genome. Because these methods rely on inducing breaks in both the genome and the array, they are mutagenic and the integrated array is not necessarily the same as its extrachromosomal progenitor. As such, there is still a need for an easy, high-efficiency, and non-mutagenic method for targeted integration of extrachromosomal arrays in *C. elegans*.

Phage have solved the problem of integrating their own DNA with high-fidelity into a host's genome using serine integrases and short DNA sequences called attachment (att) sites (*11*). Virus genomes contain a single *attP* ("phage") site; host genomes contain an *attB* ("bacterial") site. A serine integrase encoded in the phage genome mediates a unidirectional recombination between the *attP* and *attB* sites, integrating the circular phage genome. This recombination converts the *attB* and *attP* sites to *attL* ("left") and *attR* ("right"), preventing excision. The PhiC31 integrase (hereon referred to as "PhiC31"), is functional in the *C. elegans* germline. Recently, we and others have shown that PhiC31 can integrate single-copy *attP*-containing transgenes and protein tags at an *attB* site in the genome with high-efficiency (*12–14*). PhiC31 also has been shown to induce recombination between *attB* and *attP* sites located on homologous chromosomes (*13*). In this work, we show that PhiC31 can also integrate *attP*-containing extrachromosomal arrays at *attB* sites in the genome with very high efficiency. A single injection can yield a diverse collection of array sizes and compositions. We sequenced and assembled three arrays, one of them end-to-end, and found they range in length from 1.6Mb to ~18Mb. We have named this method PhIAT (pronounced "fiat") for **Ph**iC31-mediated **I**ntegration of **A**rrays of **T**ransgenes.

## Results

### Extrachromosomal arrays are integrated by PhiC31 at high efficiency.

We tested whether PhiC31 could be used to integrate arrays into a single *attB* site in the *C. elegans* genome. DNA injected into a *C. elegans* gonad is assembled into large, circular extrachromosomal arrays that can contain many copies of each constituent DNA molecule. If arrays contain many *attP* sites, PhiC31 should mediate recombination between one of the *attP* sites and a single genomic *attB* site. Applying selection to maintain the array would cause animals carrying an integration event – even if it were rare and multiple generations after injection – to increase in frequency in the population, as most extrachromosomal arrays are lost between generations at significant rates. This method is summarized in Figure 1A.

To test the method, a strain was created that contained a single *attB* site on chromosome I (near *ttTi4348*, *oxSi1337[attB] I*) and a transgene expressing PhiC31 in the germline on chromosome II (*oxSi1347[Pmex-5::PhiC31(PATC)::SL2::mNeonGreen] II*). Into this strain a mixture of linear DNA fragments was injected: a PCR product of a pan-muscle TagRFP-T transgene (*Pmlc-1::TagRFP-T*), a hygromycin-resistance selectable marker to which we appended an *attP* site by PCR (HygR::*attP*), and

stuffer DNA. Independent F1 array animals were singled and lines propagated at 25°C on hygromycin plates for about 10 generations (two rounds of starvation and chunking). After selection 8 animals per line were singled to permissive plates and screened for homozygous segregation of the RFP marker. Of the 12 lines that survived selection, 11 produced homozygous inserts (92% efficiency). The mean integration rates of arrays made from linear DNA was 91% from three independent experiments (Figure 1B).

Arrays can also be assembled from injection of circular plasmid DNA. Arrays generated from circular DNA were created in two ways: with the *attP* site and HygR on the same plasmid or on different plasmids. Both mixes used the pan-muscle TagRFP-T as a visible marker. These mixes were injected into the *attB PhiC31* strain, array-positive F1s were singled to generate lines, and selection and screening were performed as described above. Across three replicates of each experiment, arrays with a combined HygR::*attP* plasmid integrated in 61% of lines, and arrays with separate HygR and *attP* plasmids integrated in 57% of lines (Figure 1B). We confirmed the specificity of integration at the attB site on chromosome I by genetic mapping. 38 integrants were tested, and all of them mapped to chromosome I.

We confirmed that integration was dependent on PhiC31. Integration was tested in a strain containing only a genomic *attB* site ('no-PhiC31'), a strain only expressing PhiC31 ('no-*attB'*), and using an array that lacked *attP* sites ('no-*attP'*). Neither the 'no-*attB'* nor the 'no-*attP'* yielded integrations (out of 28 and 15 lines tested, respectively). Two arrays in the 'no-PhiC31' control experiment (out of 35 lines tested) yielded homozygous array insertions that did not map to the *attB* site on chromosome I (Figure 1B).

When does integration occur? Using the above selection, integration could occur at any point before we screened at about the 10th generation after injection. To test the timing of integration array(+) animals were singled every generation and integration was monitored by screening for homozygous arrays. The generation an animal carrying a homozygous array was picked is a conservative estimate for time of integration, since integration must have occurred in the germline of an animal at least two generations prior. Integrations were tracked from 15 unique array lines over the course of 12 generations (Figure 1C) Homozygous arrays were isolated from seven of the lines in the F3 generation, implying that these arrays integrated within the germlines of the F1. Three more lines integrated by the F5 generation. No integrations were isolated from the remaining five lines through the F10 generation.

Why do some arrays not integrate? To test whether the attB site could be damaged (maybe by a failed recombination) we sequenced the attB site from lines that survived selection without integrating an

array. Out of 21 non-integrating lines, 20 had mutated attB sites (Supplemental Figure 1A and 1B). Mutations were primarily small insertions or deletions consistent with a microhomology-dependent repair mechanism (*15*).

Altogether, these results show that PhIAT is efficient, integrates arrays specifically at attB sites, and happens quickly, often within the first two generations after array formation.

**Strains and DNA reagents for targeted array insertion**

To facilitate use of the method in the *C. elegans* community, we built various *attP* plasmids, as well as a set of *attB*- and PhiC31-containing strains. *attP* plasmids lacking a selection can be used in combination with any selection plasmid. We also created *attP* plasmids containing well-established drug resistance markers for hygromycin, neomycin/G418, and puromycin, as well as *unc-119(+)* rescue (Figure 2A). These plasmids were all tested and could successfully select for array integration. *attB* sites were created at safe-harbor loci on chromosomes I, II, and IV. In these strains, the *attB* sites were not marked. For PhiC31 transgenes, we tested our transgene on chromosome II (*oxSi1347*), and a transgene on chromosome IV (*jsSi1623 [Pmex-5::PhiC31::SL2::mNeonGreen] IV*, a gift from Michael Nonet*)*. Both these transgenes are capable of high-efficiency integration (File S1).

After propagating our original strain (*attB I* PhiC31 *II*) for about six months, integration stopped working; sequencing demonstrated that the *attB* site had been mutated (Supplemental Figure 1C). The mutation was a microhomology-mediated deletion, similar to those of the non-integrating lines above. Although, theoretically, PhiC31 only acts on paired attB and attP sites, at a low probability PhiC31 binding to a lone attB site appears to lead to cuts and mutation of the site. Typically, we inject directly into an *attB* PhiC31 strain. Thus, for long-term storage, it is recommended that the *attB* site and PhiC31 remain separated. A PhiC31-expressing strain can be crossed to an *attB* strain and homozygosed to reconstitute an injection strain.

To facilitate crossing, both the *attB* and PhiC31 strains were altered. We added chromosomes containing RFP linked to Him mutations (*him-8 IV* and *him-5 V*) to strains containing attB sites. Homozygous *attB* males from this strain are crossed to the PhiC31 strain. The PhiC31 strains carry a fluorescent marker that balances the *attB* site in the F1 (Figure 2B). In the F2, *attB* homozygotes will lack the balancer, PhiC31 can be homozygosed by following mNeonGreen germlines, and the Him mutation can be removed by following its linked fluorescent marker.

Do strains need to be homozygous for PhiC31 and *attB* to yield integrations? We tested whether heterozygous F1s generated in the cross above could yield integrations. Heterozygotes (*attB / mIn1 II;*

172 *jsIs623[PhiC31, mNG] / + IV*) were injected with pan-muscle TagRFP-T and HygR::*attP* and assayed for
173 array integration. Two injected animals were placed on each plate and hygromycin selection was
174 applied for two chunks of growth. 5 out of 7 lines that survived selection yielded homozygous insertions.
175 Thus, injecting F1 heterozygotes guarantees an undamaged *attB* target site with no loss in efficiency.
176
177 **Integrated arrays are diverse**
178 Independent arrays exhibit diverse compositions of transgenes (*1*), and individual arrays must be
179 carefully selected for optimal function. We tested whether integrants from a single injection also
180 generated a range of expression levels of a fluorescent transgene. 10 arrays containing pan-neuronal
181 YFP (*Psnt-1::YFP::histone*) at the *attB* site on chromosome IV were isolated from 16 array-bearing lines
182 (63%, Figure 3A). The expression levels of YFP from these arrays ranged eight-fold from the brightest
183 to dimmest arrays (Figure 3B). While the majority of YFP fluorescence was limited to neuronal nuclei,
184 the brightest arrays exhibited weak fluorescence from the commissures (Figure 3C). YFP was also
185 weakly expressed in non-neuronal nuclei in most arrays, perhaps due to leaky expression from the YFP
186 transgene, which contained a 3' UTR from the muscle-expressed gene *unc-54*.
187
188 **Long-read assemblies of integrated arrays**
189 The structure of extrachromosomal and integrated arrays has been characterized largely at the copy-
190 number level by Southern blots (*1*, *2*) and imaging (*4*). Arrays are thought to be highly repetitive, which
191 complicates assembly using short-read sequencing methods. Recently, groups have sequenced and
192 attempted to assemble arrays using long-read nanopore sequencing (*9*, *17*, *18*), though none of these
193 efforts were able to yield fully assembled array sequences. To improve assembly quality, we optimized
194 an extraction protocol for isolating high molecular weight DNA (see Methods) and performed Nanopore
195 DNA sequencing.
196
197 The RFP arrays used a commercial DNA ladder as stuffer DNA, which proved too short and repetitive
198 to be assembled (*oxIs675*, not shown). Thereafter, we used yeast genomic DNA as a stuffer for the
199 pan-neuronal YFP arrays. This DNA provided large fragments with high-sequence diversity to the array.
200 Three integrated arrays (*oxIs693, oxIs695, and oxIs691*) were chosen to span the range of expression
201 levels from the set. High molecular weight DNA was extracted and sequenced using the Oxford
202 Nanopore MinION platform (sequencing statistics can be found in Table S5). Annotated gene models of
203 each array are found in Figure 4. The length of these arrays varied from 2 Mb to 18 Mb and sequence
204 content accounted for differences in transgene expression:
205
206 ***oxIs691.*** This is the dimmest array of the set. *oxIs691* is fully assembled and 1.6Mb long and contains
207 5 full-length YFP fragments, 16 full-length HygR fragments, and 114 yeast fragments. We obtained

~279K reads longer than 10kb and fully assembled the array in the expected location on chromosome IV flanked by *attL* and *attR* sites. Yeast gDNA fragments ranged from 76-65673bp in length, with 91.5% being shorter than 1000bp. 2.3% of the array was made of HygR fragments, 1.6% was made of YFP fragments, and 96.1% was the yeast genome. Yeast fragments in the array covered 9% of the total yeast genome.

***oxIs695.*** This is the second-brightest array. *oxIs695* is ~6.8Mb long and contains 31 full-length YFP fragments, 238 full-length HygR fragments and 558 yeast fragments. We obtained 185K reads longer than 10kb and were able to assemble this array into seven contigs ranging from 335kb to 2.1Mb (N50=998kb). The array integrated in the correct location on chromosome IV flanked by *attL* and *attR* sites. Yeast gDNA fragments ranged from 45-74829bp in length; 86% were shorter 1000bp. 8.1% of the array was made of HygR fragments, 3% was made of YFP fragments, and 88.9% was the yeast genome. Yeast fragments in the array covered 31% of the total yeast genome.

***oxIs693.*** This is the brightest array. oxIs693 is ~17.9Mb long and contains 73 full-length YFP fragments, 502 full-length HygR fragments and 1446 yeast fragments. We were able to assemble this array into nine contigs ranging from 240kb to 4.4Mb (N50=2.3Mb). The array integrated in the correct location on chromosome IV flanked by *attL* and *attR* sites. Yeast gDNA fragments ranged from 43-85495bp in length; 83% were shorter 1000bp. 5.8% of the array was made of HygR fragments, 2.2% was made of YFP fragments, and 92% was the yeast genome. Yeast fragments in the array covered 55% of the total yeast genome.

Combined, fragments in three arrays came from all 16 yeast chromosomes and the mitochondrial DNA and covered 73% of the yeast genome (8.2 Mb out of 11.2 Mb). 95% of the yeast genome was found in 0-5 fragments across all three arrays, as would be expected from random incorporation of sheared genomic DNA (Supplementary Figure 2A). An identical fragment comprising a repeat unit from the yeast ribosomal DNA locus on ChrXII (XII:451,417-468,929) was present multiple times in all three arrays. This fragment was mapped 29 times in *oxIs691,* 51 times in *oxIs695*, and 9 times in *oxIs693*. Finding the rDNA multiple times in our arrays is consistent with it having a copy number of ~150 in the yeast genome (*19*) (Supplementary Figure 2B-C).

We were unable to fully assemble the two largest arrays *oxIs693* and *oxIs695* due to the presence of large duplications within the array. Each array has 21 regions longer than 50kb that are duplicated in multiple contigs (Supplemental Figure 3). Repeats are composed of multiple DNA fragments, implying that they were formed initially then duplicated during array assembly.

Arrays formed from circular DNAs consist of tandem arrays of injected DNAs, while arrays made from linear DNAs assort randomly by end-joining (*9*, *18*, *20*). At first glance, the assembly of our arrays (made from linear DNAs) is consistent with random assortment, though we noticed that the HygR fragments appeared to be clustered. We tested whether they were clustered using a Monte Carlo simulation in which the order of the fragments in the arrays were randomly assorted and then scored for whether neighbors were the same fragment type (yeast, HygR, or YFP). The HygR transgenes were significantly clustered ($p<1e-5$ in both arrays), while YFP transgenes in the array were randomly spaced ($p=0.16$ in *oxIs695* and $p=0.42$ in *oxIs693*).

**One-shot attB and array integration**

The strains constructed for this manuscript contain *attB* sites near common landing pads on chromosomes I, II, and IV. *attB* sites are short and simple to edit into the genome by injecting Cas9 ribonucleoprotein complex and a single-stranded DNA repair donor (*21*). We tested whether we could integrate an array at an arbitrary site in the genome through two sequential steps from a single injection: (1) edit an *attB* site into the genome using CRISPR reagents, then (2) integrate an array formed from co-injected DNA at that site (Figure 5A).

A PhiC31-expressing strain was injected with the CRISPR reagents to insert an *attB* site on chromosome III near the location of *oxTi444* universal mosSCI insertion site. The injection mix also contained PCR products for pan-muscle TagRFP-T and HygR::*attP*. F1 array(+) animals were cloned and selected. Of the 18 lines that survived selection, 13 yielded a homozygous array integration (72%). Genetic mapping of these insertions placed them on chromosome III consistent with being inserted at the new *attB* site. The same experiment was repeated targeting sites on chromosomes V (near the *oxTi365* universal MosSCI site) and X (within the *F40B5.5* ncRNA cluster), yielding 7 integrants from 11 lines with an insertion (64%) for chromosome V and 4 integrants from 18 lines (22%) for chromosome X (Figure 5B). These experiments show that arrays can be inserted at new *attB* sites using a single injection, albeit with lower efficiency that injecting into a strain with an existing *attB* site.

**Integration at a fluorescent landing pad**

We have focused on integrating at simple *attB* sites that are otherwise unmarked, primarily because these are very easy to knock into the genome. Because *attB*s are inert in the genome, screening for integrations can be done only by visually testing for homozygous transmission. In FLInt (*10*), another method for targeted integration, arrays are knocked into a fluorescent transgene. Integration of the array at the landing pad eliminates the landing pad's fluorescence. This provides both a positive screen (presence of the array) and negative screen (loss of landing pad fluorescence).

We implemented this strategy with our method. A new landing pad was created, containing a nuclear-localized CyOFP transgene expressed in the intestine (Figure 6). An *attB* site flanked by loxP sites (the target of Cre recombinase) was inserted within an intron in the *cyofp* gene. A single copy of this landing pad was integrated on chromosome I and crossed to a strain expressing PhiC31. This strain was injected with an array mixture containing a linear pan-muscle TagRFP-T transgene and a HygR::*attP* PCR product, and array(+) lines were selected on hygromycin as before. In addition to screening for inserts post-selection (our standard screening method), lines were examined after each chunk for array(+) CyOFP(-) animals. Out of 25 lines, integrations in 11 lines were isolated using the positive-negative visual screen (44% integration rate). One additional line integrated its array, but did not lose CyOFP fluorescence. Another line lost CyOFP fluorescence but did not integrate its array. These experiments show that arrays can be integrated into a fluorescent transgene at similar rates to integration at a “naked” *attB*, but integrants can be isolated simply by loss of fluorescence.

## Discussion

For extrachromosomal arrays to be maintained with stable expression and segregation, they must be integrated into the genome. PhIAT is a method for high-efficiency targeted integration of extrachromosomal arrays in *C. elegans.* Arrays that contain PhiC31 *attP* sites are integrated with 50-100% efficiency into a genomic *attB* site. This method is simple and can yield large numbers of diverse integrated arrays at specified loci with little researcher effort.

Currently, the best methods for targeted array integration use CRISPR to cut the genome; mosTI (*9*) and FLInt (*10*) generate integrations in 25% and 3% of array-bearing progeny, respectively. PhiC31 integrates extrachromosomal arrays with very high efficiency, greater than 90% of the array bearing lines for linear arrays. Ironically, the improved efficiency may be due to the sluggish inefficiency of PhiC31. In both FLInt and mosTI, array formation is occurring at the same time as Cas9 cleavage of the integration site. If an array isn’t formed and inserted into the cut site before the double-strand break is repaired and mutated, that line is a dead-end. Injected Cas9 ribonucleoprotein complex is short-lived and lost after the P0 generation. Plasmid reagents delivered by mosTI injection can persist through generations, but the array must have incorporated the Cas9 transgene. By contrast, in our method, the extrachromosomal arrays form after injection, and then expression of PhiC31 integrates the array at some point in subsequent generations.

Should all arrays be integrated by PhIAT? Maybe not. In our hands, PhIAT works very well for integrating arrays that do not affect the physiology of the worm (for instance, fluorescent reporters and tagged proteins). PhIAT may struggle with arrays that are toxic (whether purposefully, when overexpressing dominant negative transgenes, or incidentally, as for arrays that squelch because they

316 contain too much of a high-expression promoter like *Pmyo-2*). The method uses selection to increase
317 an integrated array's frequency in the population; selection against array toxicity fights against selection
318 for array transmission. We have not intentionally tested whether PhIAT integrates toxic arrays with high
319 efficiency, but we have isolated some arrays that cause the worm to be sick. Integrating toxic arrays
320 soon after injection is an effective strategy (*22*), so using other methods in which integration is
321 screened early will likely be more useful than PhIAT for targeted integration in these cases.
322
323 A benefit of PhIAT is the number of integrants one can isolate. Here, we isolated as many as 24 unique
324 integrated arrays from a single injection session, and we noted that integrants had diverse ratios of
325 incorporated DNA. Array diversity is important for obtaining the correct stoichiometry of transgenes. For
326 example, the composition of the NeuroPAL array, used for identifying neurons by color and position,
327 needed to be tuned to optimize expression of four fluorescent proteins across 41 transgenes (*23*). With
328 PhIAT, it seems feasible that with only moderate effort at the injection microscope, one could create
329 even hundreds of stably integrated arrays. Isolating the one perfectly stoichiometric array is only a
330 matter of screening for function.
331
332 We sequenced and assembled three integrated arrays using long-read sequencing. To our knowledge,
333 the assembly of the 1.6Mb *oxIs691* is the first end-to-end assembly of a large repetitive array (a ~35kb
334 biolistic insertion has also been assembled end-to-end using Nanopore sequencing (*17*)). We were
335 able to achieve this by improving array assembly in two ways: First, we optimized a protocol for
336 extraction of high molecular weight DNA from *C. elegans.* Good assemblies require sequencing very
337 long DNA molecules in order to scaffold repetitive contigs. Over 50% of our Nanopore reads were
338 longer than 15kb, and some were over 150kb in length, which gave us sufficient coverage to use only
339 reads longer than 50kb in our assemblies. Second, after computational assembly, we further refined
340 contigs by manual assembly using polymorphisms and incomplete DNA fragments (for example, *Psnt-*
341 *1::YFP* transgenes that did not include their histone sequences) as landmarks. Our assemblies
342 supplement the small but growing set of sequenced arrays in *C. elegans* (*9*, *18*), and provide a
343 resource to test possible mechanisms through which arrays form.
344
345 Finally, we note that the size of the arrays we and others have integrated are on the scale of whole
346 microbial genomes. In only the three arrays we sequenced and assembled, we integrated 72% of the
347 entire yeast genome into the worm genome. *C. elegans*, therefore, could be used as a crucible for
348 studying the evolution and function of genomes of other organisms, transgressing the boundaries
349 between species.
350

**Acknowledgments.** EJ is an investigator of the Howard Hughes Medical Institute. This work was supported by NIH grants R01GM095817 (to EJ) and R35GM128804 (to OR). MSR was supported by NIH grant F32GM133139. We thank the Caenorhabditis Genome Center (University of Minnesota) for strains and Wormbase for maintaining genomic and genetic data. Michael Nonet and Christian Frokjaer-Jensen provided important insight in the development of the method, and Maitreya Dunham reminded us where the yeast ribosomal DNA locus was. We thank the rest of the Jorgensen Lab for helpful suggestions for both experiments and writing.

## Figures

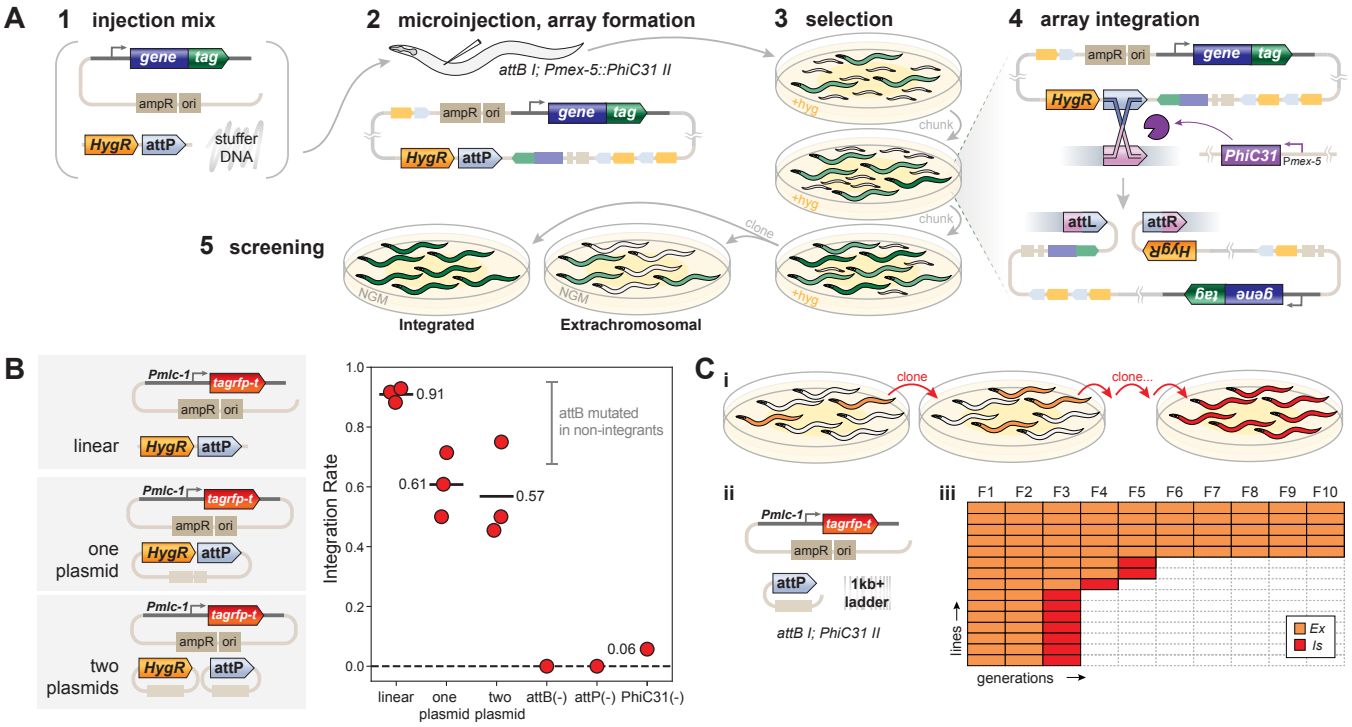


**Figure 1. A method for targeted integration of extrachromosomal arrays using PhiC31.** (A) Overview of PhIAT. (1) A DNA mixture is injected into the germline of a *C. elegans* strain that has an *attB* site in its genome and expresses PhiC31 integrase in its germline. (2) Array-positive F1s are cloned to hygromycin plates and (3) grown for multiple generations while selecting for array transmission. (4) During selection, the PhiC31 integrates the array into the genome. The generation after the array integrates, homozygous array(+) animals will be in the population and out-compete non-integrated animals. (E) After selection (in our hands, after 2-3 chunks), array(+) animals are screened for 100% transmission of the array. (B) Array integration efficiency. (left) Arrays were made by co-injecting a pan-muscle TagRFP-T transgene, a hygromycin selection, and *attP* site using either linear DNAs or plasmids. In plasmid-based integrations, the hygromycin selection and *attP* site were either contained on the same plasmid or split into different plasmids. (right) Integration rates were measured for linear and plasmid-based arrays as well as controls. Each point represents, for a single injection, the rate at which array(+) lines that survived selection yielded a homozygous integrant. The mean rate across experiments is show as a black bar. Controls used a linear injection mix. Linear: N=3 (n=12, 17, 14); one plasmid: N=3 (n=12, 23, 7); two plasmid: N=3 (n=11, 16, 20); *attB*(-): n=28; *attP*(-): n=15; PhiC31(-): n=35. (C) Array integration timing. (i) Outline of experiment. Array positive animals were cloned every generation, and their progeny screened for homozygous integrants. (ii) A linear injection mix was used in this experiment. Arrays were integrated into the *attB* site on chromosome I. (iii) A heatmap showing for each line whether the animals in that generation carried an extrachromosomal array (or non-homozygous integrant, orange) or an integrated array (red).

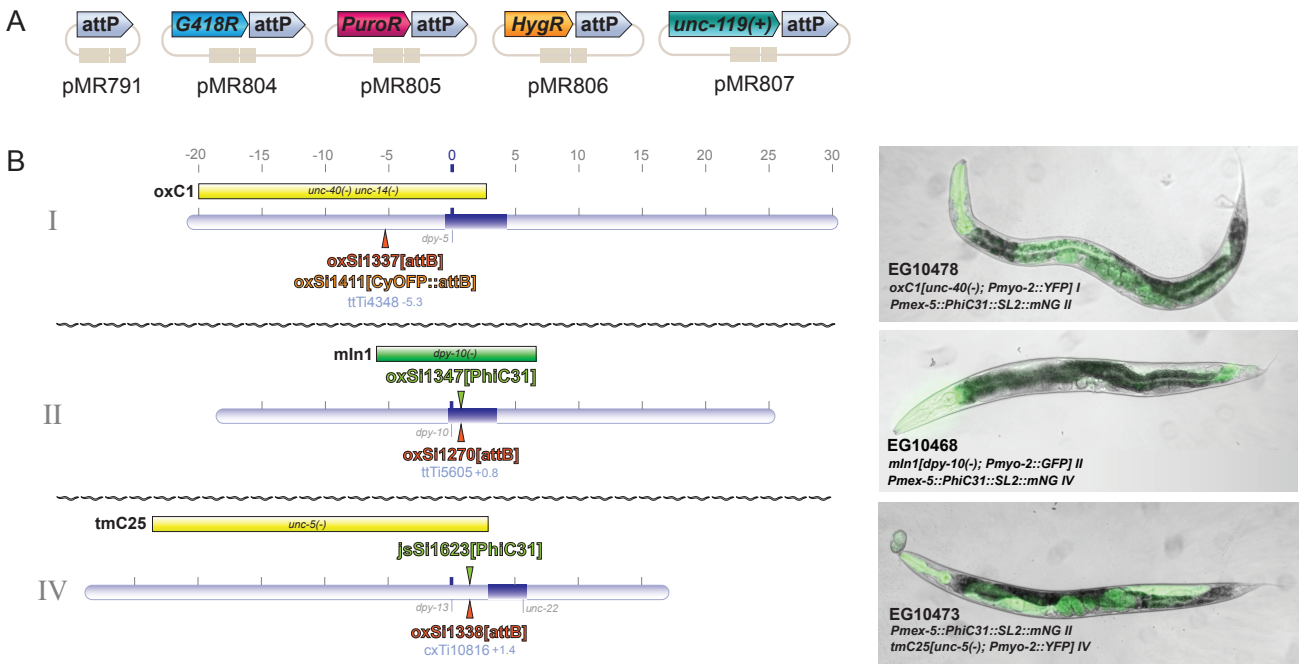


**Figure 2. A collection of plasmids and strains for PhiC31-mediated array integration.** (A) attP selection plasmids. pMR791 does not contain a selection but can be used in combination with any non-*attP* selection (e.g., *pha-1*, *lin-15*, *etc*). (B) Genetic map showing location positions of *attB* sites (orange), germline-expressed PhiC31 transgenes (green), and fluorescently-marked balancers with respect to chromosomes I, II, and IV. To the right of each chromosome is a representative image of the PhiC31(+) balancer(+) strain for each *attB* site. Fluorescence from the balancer is visible in the pharynx of each animal. In EG10478 (top) and EG10473 (bottom), mNeonGreen fluorescence marking the PhiC31 transgene (*oxSi1347 II*) is bright. In EG10438, the PhiC31 transgene (*jsSi1623 IV*) is dim and difficult to see along with bright fluorescence from the *mIn1* balancer.

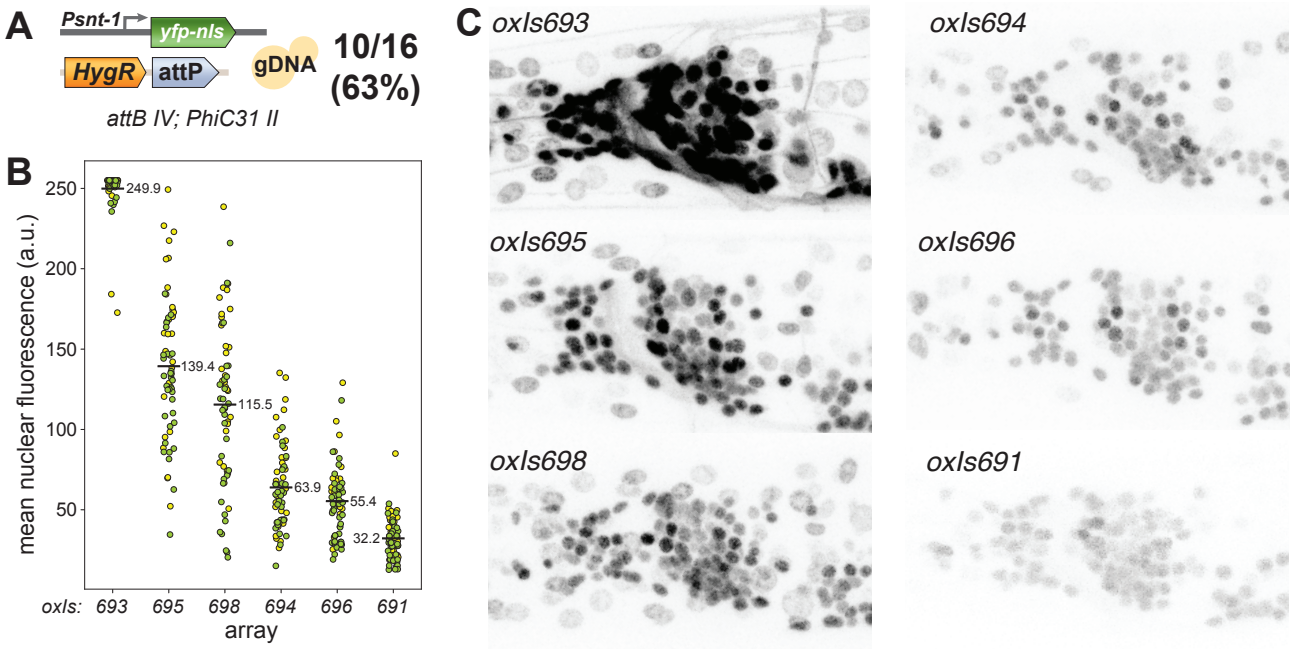


**Figure 3. PhiC31-integrated arrays are diverse.** (A) Injection mix for YFP arrays. PCR products for Psnt-1::YFP::histone and HygR::attP, along with yeast genomic DNA for stuffer, were injected into an PhiC31 II; attB IV strain. 10/16 lines that survived hygromycin selection generated integrants in this experiment. (B) Animals with integrated arrays were imaged by confocal microscopy to measure the YFP brightness of their neuronal nuclei. The brightness of nuclei in the anterior ganglion were quantified. Each point denotes a single nucleus. Colors (yellow or green) denote measurement from two individuals. The mean fluorescence across all nuclei is annotated. (C) Representative images of integrants, YFP is largely restricted to nuclei; however fluorescence from the brightest arrays (*oxIs693* and *oxIs695*) was observed in neurites. The *oxIs693*, *oxIs695*, and *oxIs691* arrays were sequenced and assembled.

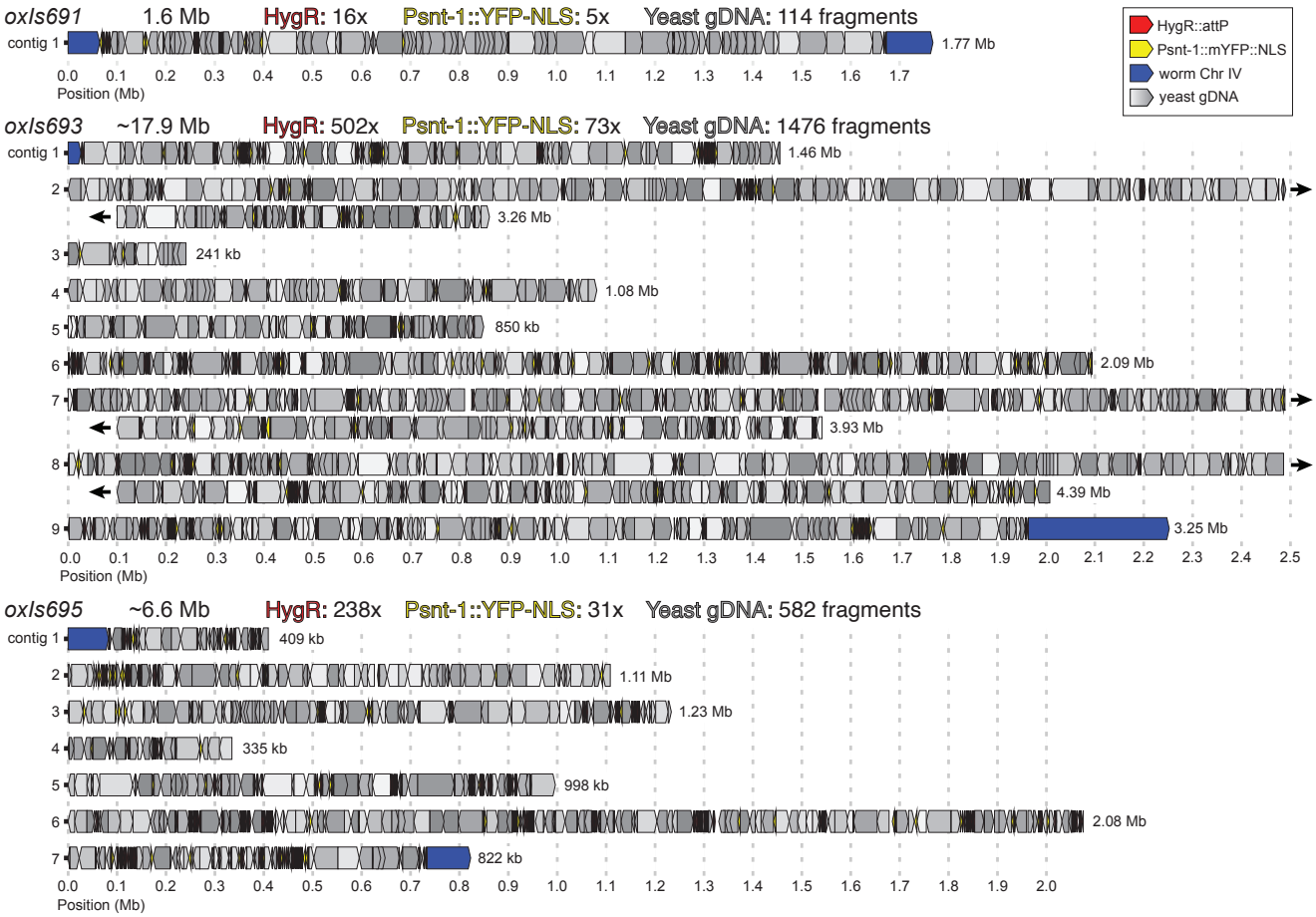


**Figure 4. Assembled integrated arrays.** Annotated contigs for *oxIs691, oxIs693, and oxIs695*. The estimated total length of each array, as well as number of constituent fragments, is written above each diagram. A single contig is drawn per line. In *oxIs693* contigs 2, 7, and 8, were too long to plot easily and were wrapped to new lines; these cases are denoted with black arrowheads. The length of each contig is noted at the end of each line. An additional megabase of *C. elegans* sequence has been truncated from the right side contig 9 in *oxIs693* for the purpose of drawing this figure. Annotations are drawn as boxes with arrows pointing in the direction of transcription (for transgenes) or based on the reference (for yeast or worm genome fragments) and are colored based on their identity (HygR: red; YFP: yellow, *C. elegans* chromosome IV: blue; yeast genomic DNA: gray, shaded based on chromosome).

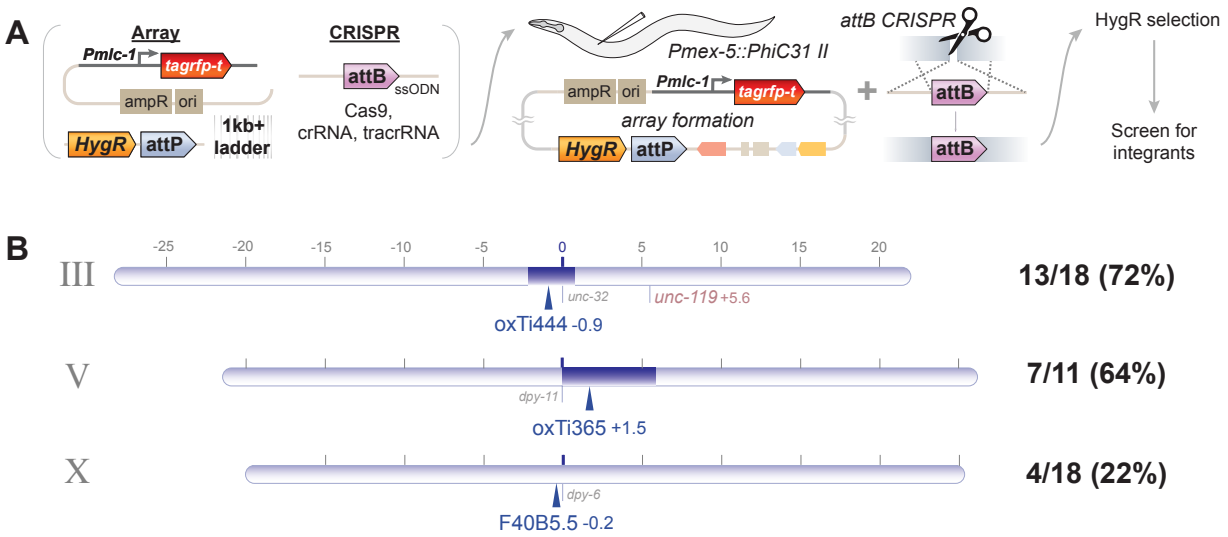


**Figure 5. attB knock-in and array integration from a single injection.** (A) Overview of method. A PhiC31(+) strain is injected with a single mix containing DNA reagents for an array and CRISPR reagents for knocking an attB site into the genome with and ssODN and Cas9 ribonucleoprotein complex. Array(+) F1 animals, which have also likely received CRISPR reagents that can insert an attB site in the genome, are cloned, selected, and screened for integrants. (B) Genetic map for three sites in the genome where we tried this method: near the oxTi444 locus on chromosome II, near the oxTi365 locus on chromosome V, and near F40B5.5 on chromosome X. The frequency at which we isolated integrants at each site is shown to the right of the chromosome.

429

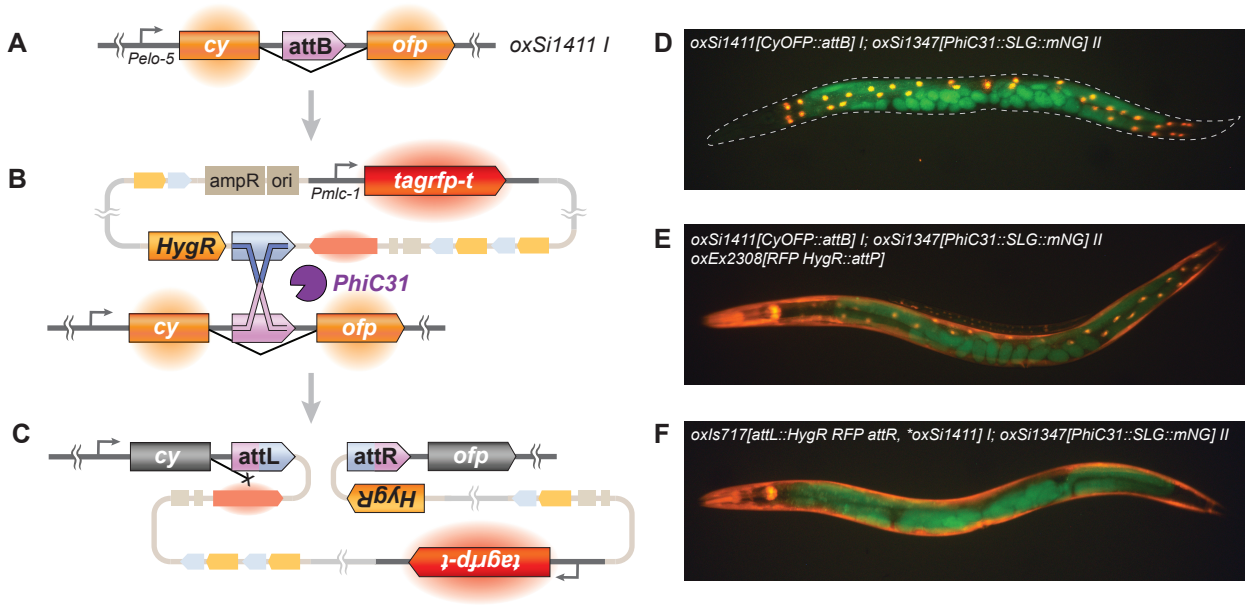


430

431 **Figure 6. Integration into a fluorescent landing pad.** (A-C) Schematic of integration into a landing
432 pad. (A) A landing pad containing an intestinally-expressed nuclear-localized CyOFP is integrated as a
433 single copy in the genome (in this case, on chromosome I). An attB site has been inserted in an early
434 intron in the transgene. (B) An extrachromosomal array (in this case, containing muscle-expressed
435 TagRFP-T attP sites and hygromycin selection) is injected into the landing pad strain. During selection,
436 PhiC31 mediates recombination between attP in the array and attB in the genome. (C) When the array
437 is integrated, it is recombined into the CyOFP intron, knocking out the fluorescence. Fluorescence from
438 the array is maintained. (D-F) Representative images of animals at each stage in the integration
439 process. In (D), CyOFP(+) intestinal nuclei can be seen. In (E), the strain carries an extrachromosomal
440 array before integration; both CyOFP(+) intestinal nuclei and TagRFP-T fluorescence from the array
441 can be seen. In (F), the array from (E) has integrated into the landing pad and is homozygous; no
442 CyOFP fluorescence is present in the intestine. Germline mNeonGreen fluorescence from the PhiC31
443 transgene is present in all images.

444

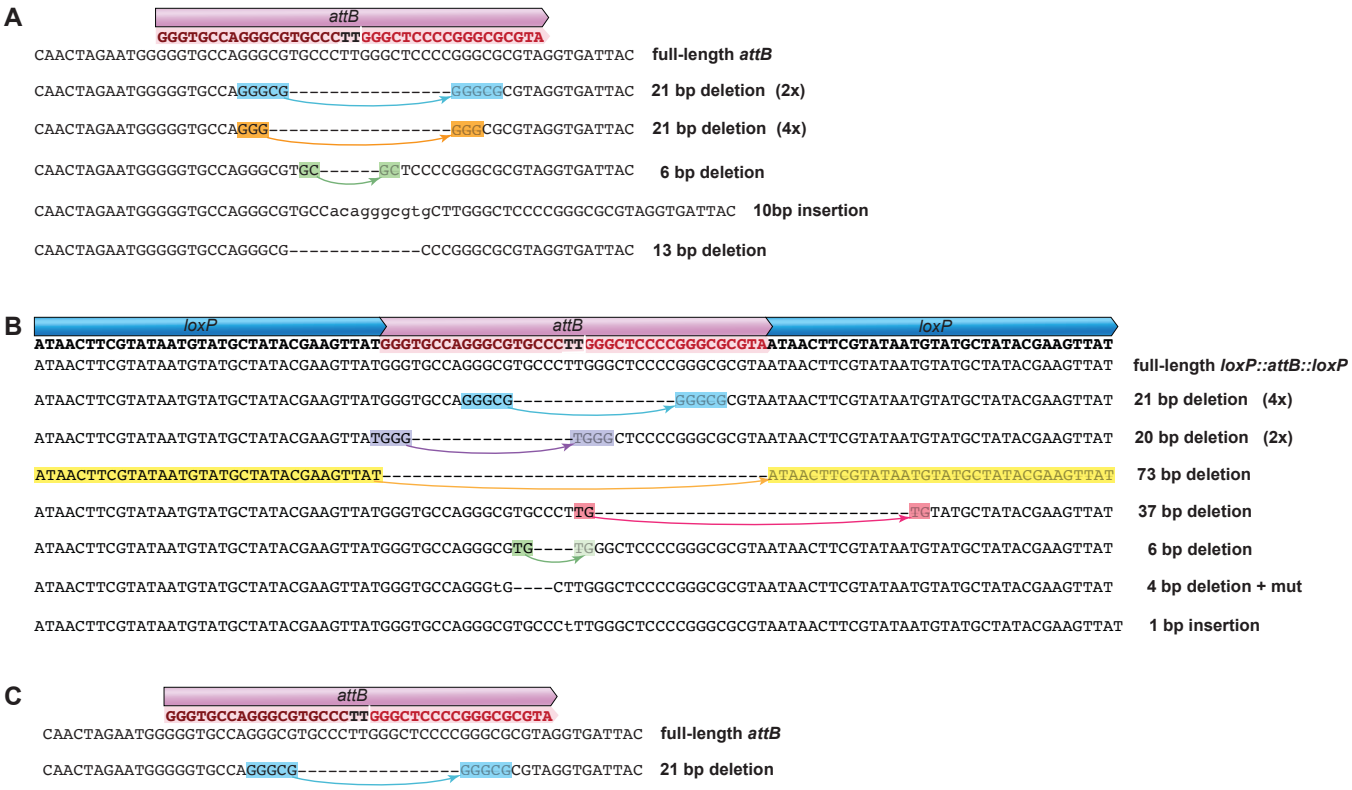


**Supplemental Figure 1. Mutated attB sites.** We sequenced the *attB* sites in strains that did not yield integrants. Each line is a different mutation to the attB site, with a description and whether it was isolated multiple times shown to the right. Most mutations were consistent with a microhomology-mediated repair causing a deletion. These repairs are annotated with colored highlights showing the relevant microhomology. Unannotated sequences do not appear to be mutated by microhomology. (A) lines from attempted integration into *oxSi1337*. (B) Lines from attempted integration into *oxSi1411*. (C) The mutation found in oxSi1337 after long-term propagation with PhiC31.

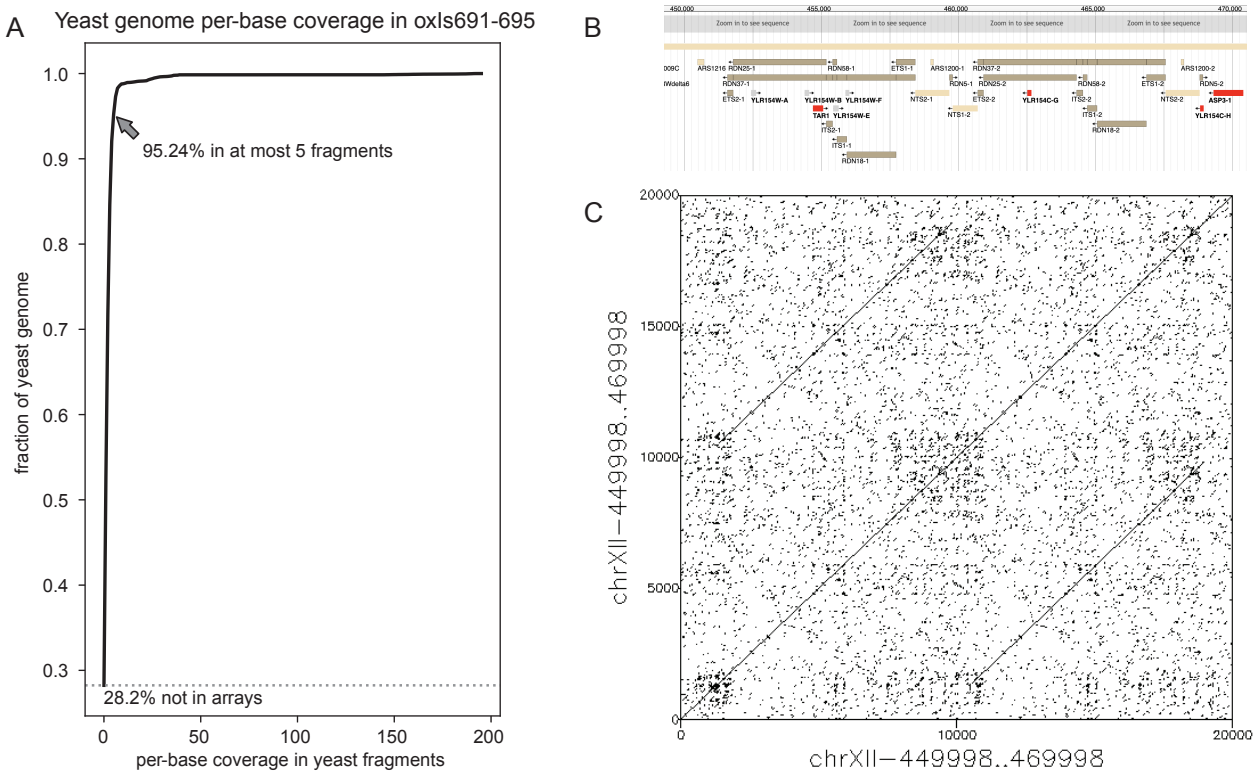


**Supplemental Figure 2. Coverage of the yeast genome in integrated arrays.** (A) Cumulative plot showing how often a base in the yeast genome is present is our arrays. 28.2% of the genome is not present in the arrays and over 95% of the yeast genome is represented in between 1 and 5 fragments across all three arrays. The long tail in the distribution up to bases found up to 195 times in the array, is caused by the repeated incorporation of the ribosomal DNA locus on ChrXII. A browser shot of the region is shown in (B). (C) A dot plot of the region. The diagonal lines in the plot denote that it is a tandem duplication. Dot plot made by dotmatcher using the following parameters: windowsize=20, threshold=40.

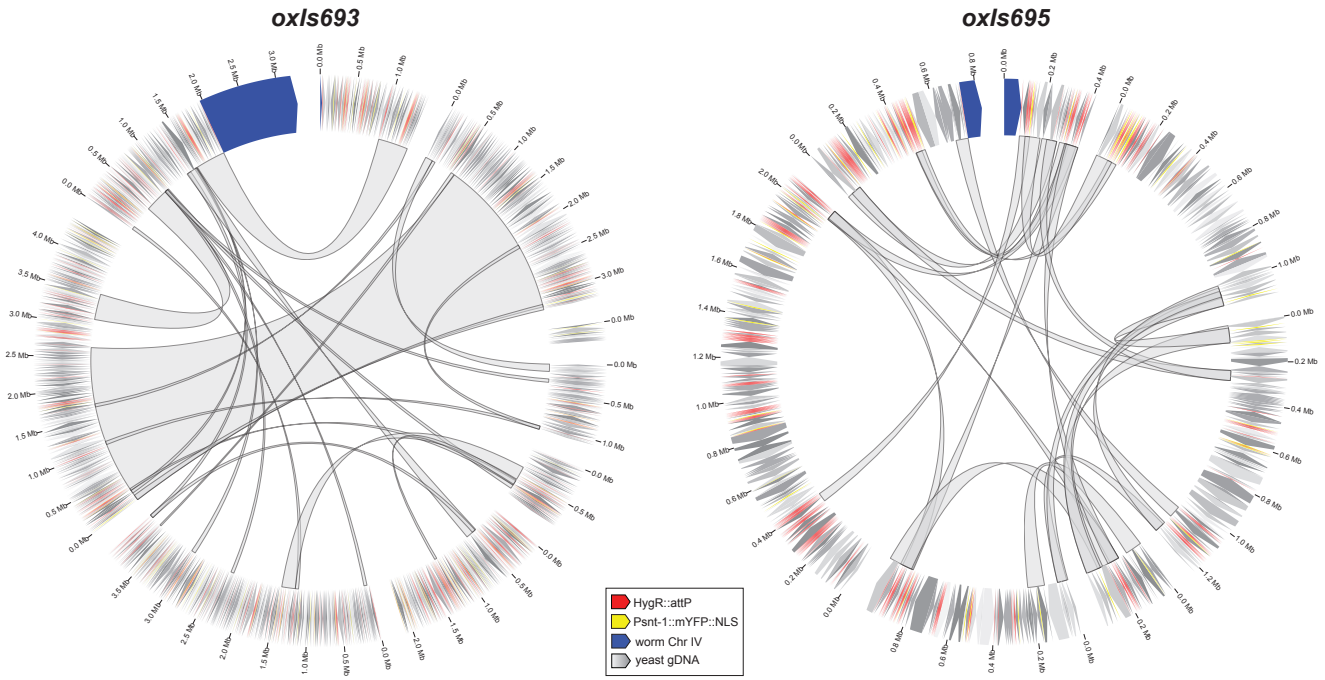


**Supplemental Figure 3. Large repeats found in integrated arrays.** Repeats that are found on multiple contigs are plotted as Circos plots for *oxIs693* (left) and *oxIs695* (right). Around the outside of the plots, the annotated array sequence is plotted as in Figure 4. Arcs inside the plot denote repeats longer than 50kb. Both arrays have 20 of these repeats. The large repeat in *oxIs693* is likely a missed merger between contigs during assembly.

## Author Contributions

*Conceptualization* MSR, EJ

*Funding Acquisition* EJ, OR

*Investigation* MSR, RP, AH

*Methodology* MSR, RP

*Writing* MR, EJ

## Materials and Methods

*Reagents*

All chemicals were purchased from Sigma-Aldrich (St. Louis). Hygromycin, G418, and puromycin were purchased from GoldBio (St. Louis). All enzymes were purchased from New England Biolabs (Beverly, MA). All synthetic DNAs were purchased from Integrated DNA Technologies.

*C. elegans strains*

*C. elegans* strains were cultured using standard methods (*24*) on nematode growth media (NGM) feeding on OP50 or HB101 bacteria. Animals were maintained at 15°C, 20°C, and 25°C. A list of worm strains created in this study can be found in Table S1. Drug plates were made by top-plating 500ul of drug (hygromycin: 4mg/ul, G418: 25mg/ul, puromycin: 10mg/ml + 0.1% Triton X-100) onto 6cm NGM+HB101 plates.

*Molecular biology and cloning*

A list of plasmids used in this study can be found in Table S2. A list of primers and RNAs used in this study can be found in Table S3. Novel plasmids were created using standard molecular biology techniques or ordered from Twist Bioscience. Annotated sequences for all plasmids can be found in Supplementary File 2.

*General injection procedures*

All injections were conducted into young adult (<48 hours) hermaphrodites raised at 15°C on HB101 bacteria. All plasmids were purified using the Qiagen miniprep kit (Qiagen). Linear DNAs were prepared either by PCR using Q5 polymerase (NEB) or plasmid digestion followed by gel extraction using the Qiagen Minelute gel extraction kit (Qiagen). Details about injection mixes used here can be found in Table S4.

*Integration method*

An injection mix containing transgene cargo, an attP-containing fragment/plasmid, a selection fragment/plasmid, and stuffer DNA was injected into young adult hermaphrodites that have an attB in

515 their genome and express PhiC31 in their germline. Stuffer DNA was either a 1kb+ DNA ladder
516 (Invitrogen #10787018) or yeast genomic DNA (Sigma-Aldrich #69240-3). Injected animals were pooled
517 2-3 per NGM plate. After three days, array(+) F1s were cloned to selective plates (or NGM plates in the
518 case of *unc-119* rescue) and grown at 25°C. When plates were close to starvation, a 1cm x 1cm chunk
519 was moved to a new selective plate. Plates can be chunked when close to starvation as many times as
520 are necessary. In this manuscript, after two chunk's-worth of growth, strains were chunked to non-
521 selective plates to grow animals for screening. The next day, 8 array(+) L2-L4 animals per line were
522 cloned to non-selective plates. Three days later these plates were screened for homozygous array(+)
523 progeny. Results from all integration experiments can be found in File S1.
524
525 *Integration without selection*
526 EG10476 and EG10469 were crossed to reconstitute an *oxSi1337[attB] I; oxSi1347[PhiC31] II* strain.
527 These animals were injected with pSEM233 (at 1ng/ul, linearized by NdeI digest), pMR791 (at 10ng/ul,
528 linearized by NotI digest) and 1kb+ DNA ladder (at 75ng/ul). F1 array(+) progeny were cloned to NGM
529 plates. Each generation (~ every three days), 4 animals from each line were cloned to new NGM plates
530 to create a set of four plates for each line. Plates from each line were screened for 100% array(+)
531 progeny at each generation.
532
533 *attB CRISPR and integration*
534 EG10408 (*oxSi1347[PhiC31] II*) was injected with Cas9 (325ng/ul final concentration, UC Berkeley QB3
535 Macrolab), tracrRNA (100 pmol, IDT), an sgRNA for an insertion site (100 pmol, IDT), an ssODN for
536 repairing with an attB site (100 pmol, IDT), and 100ng/ul of array cargo (see Table S3 for crRNA and
537 ssODN sequences). The selection and screening strategy was the same as for injection into a PhiC31,
538 attB strain: array(+) F1s were cloned to hygromycin plates and grown at 25C for cycles of starvation
539 and chunking. 8 animals for each line were then cloned to NGM plates and screened for homozygous
540 integrated arrays.
541
542 *Creation of oxC1*.
543 The recombination suppressor balancer *tmC20* balances the attB site on chromosome I. This balancer
544 has an integrated array linked to *unc-14,* but has no phenotype. In order to add a recessive mutation
545 with a visible phenotype to *tmC20,* we created a premature stop in *unc-40*. We injected EG10476
546 (*tmC20 I; oxSi1347[PhiC31] II*) with CRISPR reagents and fluorescent co-injection markers targeting
547 residue 1138 in *unc-40* and screened the progeny of array(+) F1s for *unc-40(-)* F2s. These were cloned
548 and outcrossed to N2 to (1) isolate them from the PhiC31 transgene in the injection strain background,
549 and (2) confirm that the *unc-40* mutation was linked to the Pmyo-2::YFP fluorescent marker present in
550 the balancer.

551

552 *Fluorescent imaging.*

553 Confocal images were taken using a Zeiss LSM880 using a GaAsP detector. Epifluorescent images
554 were taken on a Zeiss Axioskop compound fluorescence microscope equipped with a CoolLED pe-
555 300lite white light LED and an Amscope MF2003-BI color CMOS camera. Worms were anesthetized
556 using 50mM sodium azide before mounting on a 3% agarose pad for imaging. For images where direct
557 comparisons were required, the same imaging settings were used for all samples.

558

559 *DNA extraction for whole-genome shotgun sequencing*

560 *C. elegans* lines were grown on 10cm NGM plates seeded with HB101 bacteria. Before starvation,
561 worms were gently washed off plates with M9 and pelleted and washed 2x with M9 to remove bacteria.
562 Genomic DNA was extracted using a Qiagen DNAeasy Blood and Tissue kit (Qiagen). Whole genome
563 sequencing was performed by the Huntsman Cancer Center Genomics Core. Libraries were prepped
564 using the New England Biolabs NEBNext Ultra II FS DNA Library Prep kit (cat#E7805L) and sequenced
565 on an Illumina NovaSeq X using a paired-end 2x151cycle protocol.

566

567 *Identifying array insertions from short read sequencing*

568 FASTQ files were processed using a custom pipeline. Briefly, reads were mapped using bwa-mem (*25*)
569 to a reference comprised of the *C. elegans* genome (WS276) and plasmid sequences contained in the
570 injection mix of the sequenced strain (usually pSEM233 and pCFJ782). Mapped reads were filtered
571 using samtools (*26*) for fragments that were split between a *C. elegans* chromosome and one of the
572 plasmids. These reads were then hand-examined using IGV (*27*) to confirm the insertion site.

573

574 *DNA extraction for nanopore sequencing*

575 *C. elegans* strains were grown to starvation on a 15cm 2XYT media plate that was seeded with NA22.
576 Starved worms were rinsed off the plate into a 15mL conical with wash buffer (100mM Tris-HCl pH 8.0,
577 100mM NaCl, 20mM EDTA). To further remove any residual bacteria, worms were pelleted and washed
578 three times with wash buffer, with the middle wash including a 30-minute incubation at room
579 temperature to aid the removal of any gut bacteria. After pelleting, 50µL of worms were resuspended in
580 485µL of wash buffer and frozen at -80°C (*17*). The worms were subsequently thawed and Proteinase
581 K and SDS were then added to final concentrations of 4 mg/mL and 0.2%, respectively. Samples were
582 then incubated for 2 hours at 60°C. Following this initial digestion, 500µL of lysis buffer (100mM Tris-
583 HCl pH 8.0, 100mM NaCl, 20mM EDTA, 4mg/mL Proteinase K and 0.2% SDS) was added and the
584 sample was incubated overnight. RNAse was then added, and the sample was incubated at 30°C for
585 30 minutes. DNA was then extracted by performing a phenol-chloroform extraction and ethanol

precipitation (*28–30*). DNA quality and quantity was checked using a NanoDrop spectrophotometer and a Thermo Fisher Scientific Qubit 4 Fluorometer.

Oxford Nanopore Technologies (ONT) libraries were prepared using ONT SQK-LSK114 according to refs (*17*, *29*). All samples were sequenced to over 50x coverage (>5Gb) using the ONT MinION sequencing device based on manufacturer's instructions and previously published protocols (*17*, *29*). All basecalling was performed using the ONT MinKNOW software and the super-accurate basecalling model, with only passed reads and reads over 1kb being kept for downstream analysis. Sequencing quality was analyzed using NanoPlot (v.1.41.3) (*31*).

*Assembly of array reads*

Integrated arrays were assembled began by performing *de novo* genome assembly using Flye (v.2.9.1-b1780) (*32*) with the following parameters; --genome-size 120m --threads 56 --iterations 5 --min-overlap 10000 --asm-coverage 40. Locations of the integrated arrays were confirmed by mapping the Flye contigs to *C. elegans* reference genome (WBcel235) (*33*). The quality and completeness of each assembly was manually inspected using IGV (v.2.16.1) (*27*). When necessary, integrated array assemblies were corrected or extended using a combination of Winnowmap2 (v.2.03) (*34*) followed by Flye for polishing. More specifically, this meant mapping all reads to the integrated array contigs and checking for any soft-clipped reads in IGV that could be used to extend contigs. If the integrated array contigs could be extended, the sequences from the soft-clipped reads were then manually concatenated to the end of the contig and validated using Winnowmap2 and IGV. If correct, the new additions were polished using Flye. A similar method for elongating contigs was employed by (*35*). The sequences of the pCFJ782, pMR209, the *C. elegans* reference genome (WBcel235) (*33*), and the *S. cerevisiae* reference genome (R64-sacCer3) (*36*) were then mapped to the integrated array contigs using minimap2 (*37*). Estimates of array sizes from multi-contig assemblies was calculated as the total non-worm DNA contained within all contigs. As such, it is likely an overestimate of the actual size of the array, given that arrays are repetitive and there will be overlaps between contigs.

*Analysis of array assemblies.*

All analyses were performed using custom Python scripts (available upon request). Plots were created using matplotlib (*38*) and seaborn (*39*). To identify repeats within assemblies, contigs were aligned to each other using minimap2 using default parameters. The resulting hits were filtered for those longer than 50kb and with a mapping quality score greater than 50. Circos plots were drawn using pyCirclize (https://github.com/moshi4/pyCirclize).

1. C. C. Mello, J. M. Kramer, D. Stinchcomb, V. Ambros, Efficient gene transfer in C.elegans: extrachromosomal maintenance and integration of transforming sequences. *EMBO J* **10**, 3959–3970 (1991).

2. D. T. Stinchcomb, J. E. Shaw, S. H. Carr, D. Hirsh, Extrachromosomal DNA transformation of Caenorhabditis elegans. *Mol Cell Biol* **5**, 3484–3496 (1985).

3. K. W. Y. Yuen, K. Nabeshima, K. Oegema, A. Desai, Rapid de novo centromere formation occurs independently of heterochromatin protein 1 in C. elegans embryos. *Curr Biol* **21**, 1800–1807 (2011).

4. A. Woglar, K. Yamaya, B. Roelens, A. Boettiger, S. Köhler, A. M. Villeneuve, Quantitative cytogenetics reveals molecular stoichiometry and longitudinal organization of meiotic chromosome axes and loops. *PLOS Biology* **18**, e3000817 (2020).

5. K. W. Y. Yuen, K. Nabeshima, K. Oegema, A. Desai, Rapid de novo centromere formation occurs independently of heterochromatin protein 1 in C. elegans embryos. *Curr. Biol.* **21**, 1800–1807 (2011).

6. C. Mello, A. Fire, “Chapter 19 DNA Transformation” in *Cuenorhubditis Elegans: Modern Biologcal Analysis of an Organism*, H. F. Epstein, D. C. Shakes, Eds. (Academic Press, 1995; https://www.sciencedirect.com/science/article/pii/S0091679X08613990)vol. 48 of *Methods in Cell Biology*, pp. 451–482.

7. T. Evans, Transformation and microinjection. *WormBook*, doi: 10.1895/wormbook.1.108.1 (2006).

8. S. Yoshina, Y. Suehiro, E. Kage-Nakadai, S. Mitani, Locus-specific integration of extrachromosomal transgenes in C. elegans with the CRISPR/Cas9 system. *Biochem Biophys Rep* **5**, 70–76 (2016).

9. S. El Mouridi, F. Alkhaldi, C. Frøkjær-Jensen, Modular safe-harbor transgene insertion for targeted single-copy and extrachromosomal array integration in Caenorhabditis elegans. *G3 (Bethesda)* **12**, jkac184 (2022).

10. N. Malaiwong, M. Porta-de-la-Riva, M. Krieg, FLInt: single shot safe harbor transgene integration via Fluorescent Landmark Interference. *G3 (Bethesda)* **13**, jkad041 (2023).

11. A. C. Groth, M. P. Calos, Phage integrases: biology and applications. *J Mol Biol* **335**, 667–678 (2004).

12. F.-J. Yang, C.-N. Chen, T. Chang, T.-W. Cheng, N.-C. Chang, C.-Y. Kao, C.-C. Lee, Y.-C. Huang, S.-P. Chan, J. Wang, phiC31 integrase for recombination mediated single copy insertion and genome manipulation in C. elegans. *bioRxiv*, 2020.11.25.398784 (2020).

13. M. L. Nonet, Creation and manipulation of bipartite expression transgenes in C. elegans using phiC31 recombinase. *bioRxiv*, 2024.03.01.583017 (2024).

14. A. Hefel, K. Kruse, K. Wall, S. Jorgensen, K. H. Ng, M. S. Rich, E. M. Jorgensen, Modular gene tagging in C. elegans. *in prep.*

15. A. Sfeir, L. S. Symington, Microhomology-Mediated End Joining: A Back-up Survival Mechanism or Dedicated Pathway? *Trends Biochem Sci* **40**, 701–714 (2015).

660 16. M. Priyadarshini, J. Z. Ni, A. M. Vargas-Velazquez, S. G. Gu, C. Frøkjær-Jensen, Reprogramming
661 the piRNA pathway for multiplexed and transgenerational gene silencing in C. elegans. *Nat*
662 *Methods* **19**, 187–194 (2022).

663 17. J. R. Tyson, N. J. O'Neil, M. Jain, H. E. Olsen, P. Hieter, T. P. Snutch, MinION-based long-read
664 sequencing and assembly extends the Caenorhabditis elegans reference genome. *Genome Res*
665 **28**, 266–274 (2018).

666 18. Z. Lin, Y. Xie, W. Nong, X. Ren, R. Li, Z. Zhao, J. H. L. Hui, K. W. Y. Yuen, Formation of artificial
667 chromosomes in Caenorhabditis elegans and analyses of their segregation in mitosis, DNA
668 sequence composition and holocentromere organization. *Nucleic Acids Res* **49**, 9174–9193
669 (2021).

670 19. T. D. Petes, Yeast ribosomal DNA genes are located on chromosome XII. *Proc Natl Acad Sci U S*
671 *A* **76**, 410–414 (1979).

672 20. D. T. Stinchcomb, J. E. Shaw, S. H. Carr, D. Hirsh, Extrachromosomal DNA transformation of
673 Caenorhabditis elegans. *Molecular and Cellular Biology* **5**, 3484–3496 (1985).

674 21. A. Paix, A. Folkmann, D. Rasoloson, G. Seydoux, High Efficiency, Homology-Directed Genome
675 Editing in Caenorhabditis elegans Using CRISPR-Cas9 Ribonucleoprotein Complexes. *Genetics*
676 **201**, 47–54 (2015).

677 22. K. Noma, Y. Jin, Rapid Integration of Multi-copy Transgenes Using Optogenetic Mutagenesis in
678 Caenorhabditis elegans. *G3 (Bethesda)* **8**, 2091–2097 (2018).

679 23. E. Yemini, A. Lin, A. Nejatbakhsh, E. Varol, R. Sun, G. E. Mena, A. D. T. Samuel, L. Paninski, V.
680 Venkatachalam, O. Hobert, NeuroPAL: A Multicolor Atlas for Whole-Brain Neuronal Identification in
681 C. elegans. *Cell* **184**, 272-288.e11 (2021).

682 24. S. Brenner, The genetics of Caenorhabditis elegans. *Genetics* **77**, 71–94 (1974).

683 25. H. Li, R. Durbin, Fast and accurate short read alignment with Burrows-Wheeler transform.
684 *Bioinformatics* **25**, 1754–1760 (2009).

685 26. H. Li, B. Handsaker, A. Wysoker, T. Fennell, J. Ruan, N. Homer, G. Marth, G. Abecasis, R. Durbin,
686 1000 Genome Project Data Processing Subgroup, The Sequence Alignment/Map format and
687 SAMtools. *Bioinformatics* **25**, 2078–2079 (2009).

688 27. J. T. Robinson, H. Thorvaldsdottir, D. Turner, J. P. Mesirov, igv.js: an embeddable JavaScript
689 implementation of the Integrative Genomics Viewer (IGV). *Bioinformatics* **39**, btac830 (2023).

690 28. J. Tyson, Rocky Mountain adventures in Genomic DNA sample preparation, ligation protocol
691 optimisation / simplification and Ultra long read generation v1. [Preprint] (2019).
692 https://doi.org/10.17504/protocols.io.7euhjew.

693 29. B. Y. Kim, J. R. Wang, D. E. Miller, O. Barmina, E. Delaney, A. Thompson, A. A. Comeault, D.
694 Peede, E. R. R. D'Agostino, J. Pelaez, J. M. Aguilar, D. Haji, T. Matsunaga, E. E. Armstrong, M.
695 Zych, Y. Ogawa, M. Stamenković-Radak, M. Jelić, M. S. Veselinović, M. Tanasković, P. Erić, J.-J.
696 Gao, T. K. Katoh, M. J. Toda, H. Watabe, M. Watada, J. S. Davis, L. C. Moyle, G. Manoli, E.
697 Bertolini, V. Košťál, R. S. Hawley, A. Takahashi, C. D. Jones, D. K. Price, N. Whiteman, A. Kopp,
698 D. R. Matute, D. A. Petrov, Highly contiguous assemblies of 101 drosophilid genomes. *Elife* **10**,
699 e66405 (2021).

30. M. Ashburner, K. G. Golic, R. S. Hawley, *Drosophila: A Laboratory Handbook* (Cold Spring Harbor laboratory press, Cold Spring Harbor (N.Y.), Second ed., 2005).

31. W. De Coster, R. Rademakers, NanoPack2: population-scale evaluation of long-read sequencing data. *Bioinformatics* **39**, btad311 (2023).

32. M. Kolmogorov, J. Yuan, Y. Lin, P. A. Pevzner, Assembly of long, error-prone reads using repeat graphs. *Nat Biotechnol* **37**, 540–546 (2019).

33. T. W. Harris, J. Baran, T. Bieri, A. Cabunoc, J. Chan, W. J. Chen, P. Davis, J. Done, C. Grove, K. Howe, R. Kishore, R. Lee, Y. Li, H.-M. Muller, C. Nakamura, P. Ozersky, M. Paulini, D. Raciti, G. Schindelman, M. A. Tuli, K. Van Auken, D. Wang, X. Wang, G. Williams, J. D. Wong, K. Yook, T. Schedl, J. Hodgkin, M. Berriman, P. Kersey, J. Spieth, L. Stein, P. W. Sternberg, WormBase 2014: new views of curated biology. *Nucleic Acids Res* **42**, D789-793 (2014).

34. C. Jain, A. Rhie, N. F. Hansen, S. Koren, A. M. Phillippy, Long-read mapping to repetitive reference sequences using Winnowmap2. *Nat Methods* **19**, 705–710 (2022).

35. K. Ichikawa, M. J. Shoura, K. L. Artiles, D.-E. Jeong, C. Owa, H. Kobayashi, Y. Suzuki, M. Kanamori, Y. Toyoshima, Y. Iino, A. E. Rougvie, L. Wahba, A. Z. Fire, E. M. Schwarz, S. Morishita, CGC1, a new reference genome for Caenorhabditis elegans. *bioRxiv*, 2024.12.04.626850 (2024).

36. S. R. Engel, F. S. Dietrich, D. G. Fisk, G. Binkley, R. Balakrishnan, M. C. Costanzo, S. S. Dwight, B. C. Hitz, K. Karra, R. S. Nash, S. Weng, E. D. Wong, P. Lloyd, M. S. Skrzypek, S. R. Miyasato, M. Simison, J. M. Cherry, The reference genome sequence of Saccharomyces cerevisiae: then and now. *G3 (Bethesda)* **4**, 389–398 (2014).

37. H. Li, Minimap2: pairwise alignment for nucleotide sequences. *Bioinformatics* **34**, 3094–3100 (2018).

38. J. D. Hunter, Matplotlib: A 2D Graphics Environment. *Comput. Sci. Eng.* **9**, 90–95 (2007).

39. M. Waskom, seaborn: statistical data visualization. *JOSS* **6**, 3021 (2021).